EJTP **3, No. 12** (2006) 19–35 *Electronic Journal of Theoretical Physics*

High-Dimensional Dynamics in the Delayed Hénon Map

J. C. Sprott*

Department of Physics, University of Wisconsin, Madison, WI 53706, USA

Received 3 April 2006, Accepted 16 August 2006, Published 20 September 2006

Abstract: A variant of the Hénon map is described in which the linear term is replaced by one that involves a much earlier iterate of the map. By varying the time delay, this map can be used to explore the transition from low-dimensional to high-dimensional dynamics in a chaotic system with minimal algebraic complexity, including a detailed comparison of the Kaplan-Yorke and correlation dimensions. The high-dimensional limit exhibits universal features that may characterize a wide range of complex systems including the spawning of multiple coexisting attractors near the onset of chaos.

Keywords: Delayed Hénon Map, Dynamical systems, Chaos, Bifurcations
PACS (2006): 05.45.-a, 05.45.Pq , 05.45.Gg, 05.45.Jn, 05.45.Ac, 05.45.Pq,45.30.+s, 05.45.-a

1. Introduction

The behavior of low-dimensional chaotic maps and flows has been extensively studied and characterized [1]. Hence, much of the interest in nonlinear dynamics is now turning to an understanding of the high-dimensional complex systems that characterize most of the real world. The intuition that has arisen from the study of low-dimensional systems does not necessarily extend to high-dimensional systems whose behavior is often quite different and in some ways simpler.

The goal of this paper is to explore the transition from low-dimensional to high-dimensional dynamics in a particularly simple example of an iterated map that is a variant of the familiar Hénon map [2]. The dynamics will be governed by a single parameter whose value determines the dimension of the system and hence its complexity. The system is algebraically minimal in that it has a single (quadratic) nonlinearity and a single linearity.

* Tel: +1-608-263-4449; fax: +1-608-262-7205
E-mail: sprott@physics.wisc.edu.

2. Delayed Hénon map

The system considered here is the time-delayed Hénon map given by

$$x_n = 1 - ax_{n-1}^2 + bx_{n-d} \tag{1}$$

For $d = 2$, this map is the familiar two-dimensional dissipative Hénon map whose solutions are chaotic for typical values of $a = 1.4$ and $b = 0.3$. This system can also be viewed as a quadratic map with time-delayed linear feedback in which d is a measure of the delay time, such as might be encountered in a chaos control scheme [3].

For $d = 1$, the map is equivalent to the one-dimensional logistic map [4]

$$y_n = Ay_{n-1}(1 - y_{n-1})$$

as is evident from the transformation

$$y = ax/A + 1/2 - b/2A$$

with the condition

$$A^2 - 2A + (2b - b^2 - 4a) = 0$$

from which it follows that a given choice of the parameters a and b maps into A according to

$$A = 1 \pm \sqrt{1 - 2b + b^2 + 4a} \tag{2}$$

3. Fixed Points

Equation (1) has fixed point solutions at

$$x_\pm = \frac{b-1}{2a} \pm \frac{1}{2a}\sqrt{(b-1)^2 + 4a}$$

These fixed points are born simultaneously in a saddle-node (blue-sky) bifurcation [5] at $a = -(b-1)^2/4$ with the smaller one (x_-) initially unstable and the larger one (x_+) initially stable. Thus for fixed b, the quantity a can be used as a bifurcation parameter to take the system from a stable fixed point into chaos, analogous to the A in the logistic map as suggested by Eq. (2).

4. Regions of Various Dynamical Behaviors

Figure 1 shows the regions of various dynamical behaviors for Eq. (1) in the ab-plane as determined numerically for various values of d. For this purpose, the initial conditions were taken as the mean of the two fixed points $x_0 = (b-1)/2a$, and the regions of chaos were identified by calculating the largest Lyapunov exponent using a variant of the Wolf algorithm [6]. There is no guarantee that a different initial condition would not produce a different dynamic in the various regions, but a full study of the basins of attractions for

every (a, b, d) combination is computationally infeasible and unessential for the purposes of this paper (however, see Section 7 below where it is shown that multiple coexisting attractors are common only near the onset of chaos).

From plots such as Fig. 1, it was determined that the values $a = 1.6$ and $b = 0.1$, as shown by the dotted lines in the figure, give chaotic solutions for all $d \geq 1$. These values are close to the largest value of b for which chaos exists for fixed a (the actual value is closer to $a = 1.5933$ and $b = 0.10834$). For much of what follows, these values will be assumed except where describing the routes to chaos, in which case b will be fixed at 0.1 and a varied over the range 0 to 2. For $d = 1$, according to Eq. (2), this choice corresponds to varying A in the logistic map from 1.9 to 3.968164416..., with the value of $a = 1.6$ corresponding to $A = 3.685144316...$, which coincidentally is very near the Misiurewicz point [7] at $A = 3.678573510...$ where two chaotic bands coalesce into one.

5. Attractors

Figure 2 shows the attractors for the system in Eq. (1) with $a = 1.6$ and $b = 0.1$ for several values of d. The global structure is dominated by the quadratic map as expected for the small value of b [8], but the dimension of the attractor clearly increases with increasing d. This increase can be quantified by calculating the Kaplan-Yorke dimension D_{KY} [9] from the spectrum of Lyapunov exponents as shown in Fig. 3 along with three of the Lyapunov exponents. Linear least-squares fits to these results over the range $1 \leq d \leq 100$ give

$$D_{KY} \cong 0.192d + 0.699$$

$$\lambda_1 \cong 0.354 - 2.3 \times 10^{-5} d$$

For these values of a and b, there is a single positive Lyapunov exponent (no hyperchaos), and the sum of the exponents is $\Sigma\lambda_i = \log|b| = -2.302585093...$ for all $d \geq 2$. Consequently, the other Lyapunov exponents tend to cluster at small negative values ($\lambda_i \sim -2.65/d$ for $2 \leq i \leq d$) in the limit of large d. The actual mean at d= 100 is –0.0268 with a standard deviation of ± 0.0049.

The metric entropy, which by Pesin's identity [10] is the sum of the positive Lyapunov exponents, is one measure of the complexity and is identical to λ_1 and nearly independent of d [11]. The single positive Lyapunov exponent is presumably a consequence of the fact that all the stretching and folding occur along a single direction in the d-dimensional state space. Note that all the exponents in this paper are base-e.

Because of the very smooth and predictable near linear variation of the attractor dimension with d, this system provides a perfect opportunity for a critical comparison of the Kaplan-Yorke dimension with the correlation dimension. Figure 3 includes data with error bars for the correlation dimension D_C [12] determined by the extrapolation method of Sprott and Rowlands [13]. Such an extrapolation is crucial for accurately calculating

these high correlation dimensions. A linear least-squares fit to the correlation dimension data over the range $1 \leq d \leq 35$ gives

$$D_C \cong 0.189d + 0.560$$

which suggests that $D_C \cong 0.981 D_{KY} - 0.126$ in keeping with the theoretical expectation [14-16] of

$$D_C \leq D_I = D_{KY}$$

where D_I is the information dimension. Similar behavior has been reported in an extensive survey of 3-dimensional chaotic systems by Chlouverakis and Sprott [17], and the results here can be viewed as an extension of that work up to $d = 35$. Such a careful comparison of these two dimensions over such a wide range is apparently a new result.

6. Routes to Chaos

It is well known that the logistic map and the Hénon map exhibit a period-doubling route to chaos as shown in the left panel of Fig. 4 for $d = 2$ and $b = 0.1$. Also typical of low-dimensional maps is the existence of dense stable periodic windows in the chaotic regime as evidenced by the negative value of λ_1 and a Kaplan-Yorke dimension of zero.

By contrast, the high-dimensional case in the right panel of Fig. 4 with $d = 100$ and $b = 0.1$ shows a much smoother transition into chaos and a complete absence of periodic windows, although there are several period doublings before the onset of chaos. A curious feature is the oscillation between simple chaos (with $\lambda_2 < 0$) and hyperchaos (with $\lambda_2 > 0$) with increasing a in the chaotic ($\lambda_1 > 0$) regime. The high-dimensional case also shows a lack of superstable orbits where λ_1 is infinitely negative. The absence of periodic windows for large d thus relates more to the dimension of the attractor than to the presence of hyperchaos in contrast to the conjecture by Thomas, *et al.* [18]. Similar behavior has been observed in delay differential equations [19], convection models governed by partial differential equations [20], lattices of coupled logistic maps [21, 22], artificial neural networks [23], and competitive Lotka-Volterra models [24].

The detailed behavior of this case near the onset of chaos is shown in Fig. 5. At a value of $a = 1.10$, the system has already period-doubled twice and exhibits a 4-cycle. When a reaches about 1.10893 without further period doubling, a Neimark-Sacker bifurcation [25, 26] occurs, leading to the appearance of a drift ring (a 2-torus in the corresponding flow) as evidenced by $\lambda_1 = 0$ and $D_{KY} = 1$. The drift ring undergoes successive period doublings, followed by a finite region of chaos with $\lambda_1 > \lambda_2 = 0$ beginning about $a = 1.13577$ before the onset of hyperchaos with $\lambda_1 > \lambda_2 > 0$. One of the Lyapunov exponents tends to remain at zero even after the onset of chaos, suggesting the existence of a neutrally stable global manifold even in the presence of chaos and hyperchaos.

The route to chaos is exhibited differently by the attractors in Fig. 6. The plot of x_n versus x_{n-50} in the upper left is a zoom into the vicinity of one of the points in the four-cycle just after the Neimark-Sacker bifurcation occurs. The succession of images shows

a circular drift ring growing to a rectangular shape and then period-doubling before the onset of chaos. The bifurcations of the drift ring to periods 2, 4, and 8 occur at $a \cong 1.12991$, 1.134524, and 1.1357040, respectively, implying a Feigenbaum number of 3.91 ± 0.01, which is similar to but possibly different from the value of $\delta = 4.669201609\ldots$ for unimodal maps with a quadratic maximum [27]. Note that the plots indicate a homoclinic tangle [28] near the corners of the rectangle as the onset of chaos is approached.

7. Global Bifurcations

The study of global bifurcations and multiple attractors in high-dimensional systems is still in its infancy [29, 30]. The system described here provides an opportunity to study such bifurcations in a particularly simple mapping. For this purpose, we characterize an attractor by a single scalar value

$$\langle r^2 \rangle = \lim_{N\to\infty} \frac{1}{N} \sum_{n=1}^{N} (x_n - x_{ref})^2 \tag{3}$$

which is the mean square deviation (the variance) of the attractor from the reference point x_{ref} projected onto one axis of the time-delay embedding space. Except for a set of measure zero, any choice of x_{ref} will give a unique and different value of $\langle r^2 \rangle$ for each attractor. For fixed parameters and many different initial conditions, multiple coexisting attractors will be indicated by values of $\langle r^2 \rangle$ that cluster around distinct values. With two different reference points, even the small potential degeneracy could be resolved by plotting the respective values in a plane, with each attractor having values that cluster near a point in the plane. Abrupt changes in the value or slope of $\langle r^2 \rangle$ as a parameter is varied will indicate a discontinuous (catastrophic or subcritical) or continuous (subtle or supercritical) bifurcation, respectively. For the study here, the reference point was taken as $x_{ref} = b/2a$ (the minimum of the parabola in Eq. (1)) and initial conditions were chosen from a normal random distribution with mean x_{ref} and variance 1.0, although other choices give similar results.

Figure 7 shows $\langle r^2 \rangle$ versus a for $b = 0.1$ and $b = 0.3$ with $d = 100$. For the smaller value of b, there is a single attractor for all values of a, but for $b = 0.3$, there is a range of a from about 0.4 to 0.8 where multiple attractors coexist, and they are most numerous near the onset of chaos. Figure 8 shows the relative probability for 8000 cases with various values of $\langle r^2 \rangle$ for $0.6 < \langle r^2 \rangle < 0.73$ with $a = 0.7$, $b = 0.3$, and $d = 100$, indicating the presence of at least seven distinct attractors. A closer examination indicates that each of these seven cases is really a cluster of distinct but similar attractors, totaling at least sixteen cases. Some of these attractors have very small basins of attraction since they occur infrequently or have very similar values of $\langle r^2 \rangle$, which makes it difficult to be confident that they are distinct.

Figure 9 shows four of the most common of these coexisting attractors. Three of them are weakly chaotic ($\lambda_1 \sim 0.002$), but the one in the upper right is a period-4 drift ring with $\lambda_1 < 10^{-8}$ (and presumably zero). Some of the attractors, such as the two at the

bottom of Fig. 9, look almost identical but are clearly distinct, as evident by the very different values of $\langle r^2 \rangle$ and the largest Lyapunov exponent.

This behavior may represent a new route to chaos through "attractor spawning." Figure 7 indicates that these attractors appear gradually as their basins of attraction grow slowly or as they gradually separate from one another. The attractors coalesce into a single strange attractor once the chaos is fully developed, and all bounded orbits then have initial conditions that lie within its basin of attraction.

Of course Eq. (3) is only one of many possible ways to characterize an attractor. The largest Lyapunov exponent λ_1 could serve as another, and its value for each of the four attractors is shown in Fig. 9. However, it is more difficult to calculate, and it tends to converge more slowly. Furthermore, it would be useless for distinguishing quasiperiodic attractors (tori) since they all have $\lambda_1 = 0$. The full spectrum of Lyapunov exponents could also be used to characterize an attractor, but that would be even more computationally demanding.

8. Summary

Simple systems such as the one described here are useful for exploring the transition from low-dimensional and high-dimensional chaotic systems. The characteristic intricate bifurcation structure and periodic windows in the midst of chaos gives way to a smoother variation and more robust behavior as the dimension increases, especially in the chaotic regime. The Kaplan-Yorke dimension increases linearly with system dimension, but the largest Laypunov exponent and metric entropy remain relatively constant. The correlation dimension is a relatively constant fraction of about 98% of the Kaplan-Yorke dimension. The period-doubling route to chaos that is common at low dimension transitions to a quasiperiodic route as the dimension increases. A method for identifying global bifurcations is described, and it shows the existence of a large number of coexisting attractors near the onset of chaos, suggesting a new route to chaos in high-dimensional systems.

Acknowledgments

Discussions with David Albers, Konstantinos Chlouverakis, and Morris Hirsch are gratefully acknowledged.

References

[1] J. C. Sprott, Chaos and Time-Series Analysis, Oxford University Press, Oxford (2003).

[2] M. Hénon, A two-dimensional mapping with a strange attractor, Comm. Math. Phys. 50 (1976) 69-77.

[3] T. Buchner and J. J. Zebrowski, Logistic map with a delayed feedback: Stability of a discrete time-delay control of chaos, Phys. Rev. E 63 (2001) 016210 [7 pages].

[4] R. May, Simple mathematical models with very complicated dynamics, Nature 261 (1976) 45-67.

[5] R. H. Abraham and C. D. Shaw, Dynamics: the geometry of behavior, Part 4: bifurcation behavior, Aerial Press, Santa Cruz, CA, (1988).

[6] A. Wolf, J. B. Swift, H. L. Swinney, and J. A. Vastano, Determining Lyapunov exponents from a time series, Physica D 16 (1985) 285-317.

[7] M. Misiurewicz, Absolutely continuous measures for certain maps of an interval, Publ. Math. I.H.E.S. 53 (1981) 17-51.

[8] G. Rowlands, Non-linear Phenomena in Science and Engineering, Horwood, Chichester (1990).

[9] J. Kaplan and J. Yorke, Chaotic behavior of multidimensional difference equations, In Functional differential equations and approximations of fixed points, Lecture Notes in Mathematics, Vol. 730 (ed. H. –O. Peitgen and H. –O. Walther), pp. 228-237, Springer, Berlin (1979).

[10] Ya. B. Pesin, Characteristic Lyapunov exponents and smooth ergodic theory, Russian Mathematical Surveys 32 (1977) 55-114.

[11] E. F. Manffra, H. Kant, and W. Just, Periodic orbits and topological entropy of delayed maps, Phys. Rev. E. (2001) 046203 [6 pages]

[12] P. Grassberger and I. Procaccia, Characterization of strange attractors, Phys. Rev. Lett. 50 (1983) 346-349.

[13] J. C. Sprott and G. Rowlands, Improved correlation dimension calculation, International Journal of Bifurcation and Chaos 11 (2001) 1861-1880.

[14] J. D. Farmer, E. Ott, and J. A. Yorke, The dimension of chaotic attractors, Physica D 7 (1983) 153-180.

[15] L. -S. Young, Dimension, entropy, and Lyapunov exponents in differentiable dynamical systems, Physica A 124 (1984) 639-646.

[16] F. Ledrappier and L. -S. Young, The metric entropy of diffeomorphisms, Annals of Mathematics 2 (1985) 509-574.

[17] K. E. Chlouverakis and J. C. Sprott, A comparison of correlation and Lyapunov dimensions, Physica D 200 (2004) 156-164.

[18] R. Thomas, V. Basios, M. Eiswirth, T. Kruel, and O. E. Rössler, Hyperchaos of arbitrary order generated by a single feedback circuit, and the emergence of chaotic walks, Chaos 14 (2004) 669-674.

[19] J. D. Farmer, Chaotic attractors of an infinite-dimensional dynamical system, Physica D 4 (1982) 366-393.

[20] H. Chaté and P. Manneville, Transition to turbulence via spatiotemporal intermittency, Phys. Rev. Lett. 58 (1987) 112-115.

[21] P. Grassberger, Information content and predictability of lumped and distributed dynamical systems, Physica Scripta 40 (1989) 346-353.

[22] K. Kaneko, Supertransients, spatiotemporal intermittency and stability of fully developed spatiotemporal chaos, Phys. Lett. A 149 (1990) 105-112.

[23] D. J. Albers, J. C. Sprott, and W. D. Dechert, Routes to chaos in neural networks with random weights, International Journal of Bifurcation and Chaos 8 (1998) 1463-1478.

[24] J. C. Sprott, J. C. Wildenberg, and Y. Azizi, A simple spatiotemporal chaotic Lotka-Volterra model, Chaos, Solitons and Fractals 26 (2005) 1035-1043.

[25] J. Neimark, On some cases of periodic motions depending on parameters, Doklady Akademii nauk Souiza Sovetskikh Skotsialisticheskikh Respuplik 129 (1959) 736-739.

[26] R. S. Sacker, A new approach to the perturbation theory of invariant surfaces, Communications on Pure and Applied Mathematics 18 (1965) 717-732.

[27] M. J. Feigenbaum, Quantitative universality for a class of nonlinear transformations, J. Stat. Phys. 19 (1978) 24-52.

[28] H. Poincaré, Analyse des travaux scientifiques de Henri Poincaré faites par lui-même, Acta Mathematica 38 (1921) 1-135.

[29] S. Wiggins, Introduction to Applied Nonlinear Dynamical Systems and Chaos, Springer, New York (1990).

[30] Y. A. Kuznetsov, Elements of Applied Bifurcation Theory (2^{nd} ed.), Springer, New York (1995).

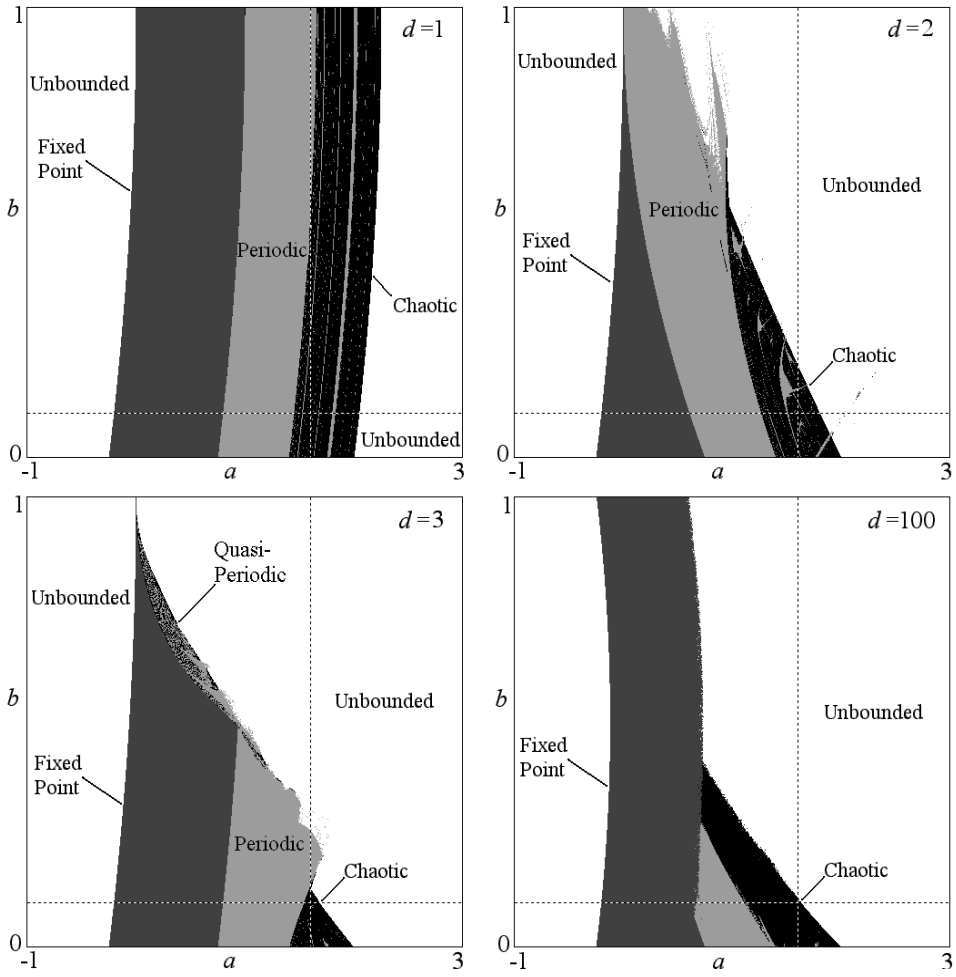

Fig. 1 Regions of dynamical behaviors for Eq. (1) for various values of the time delay.

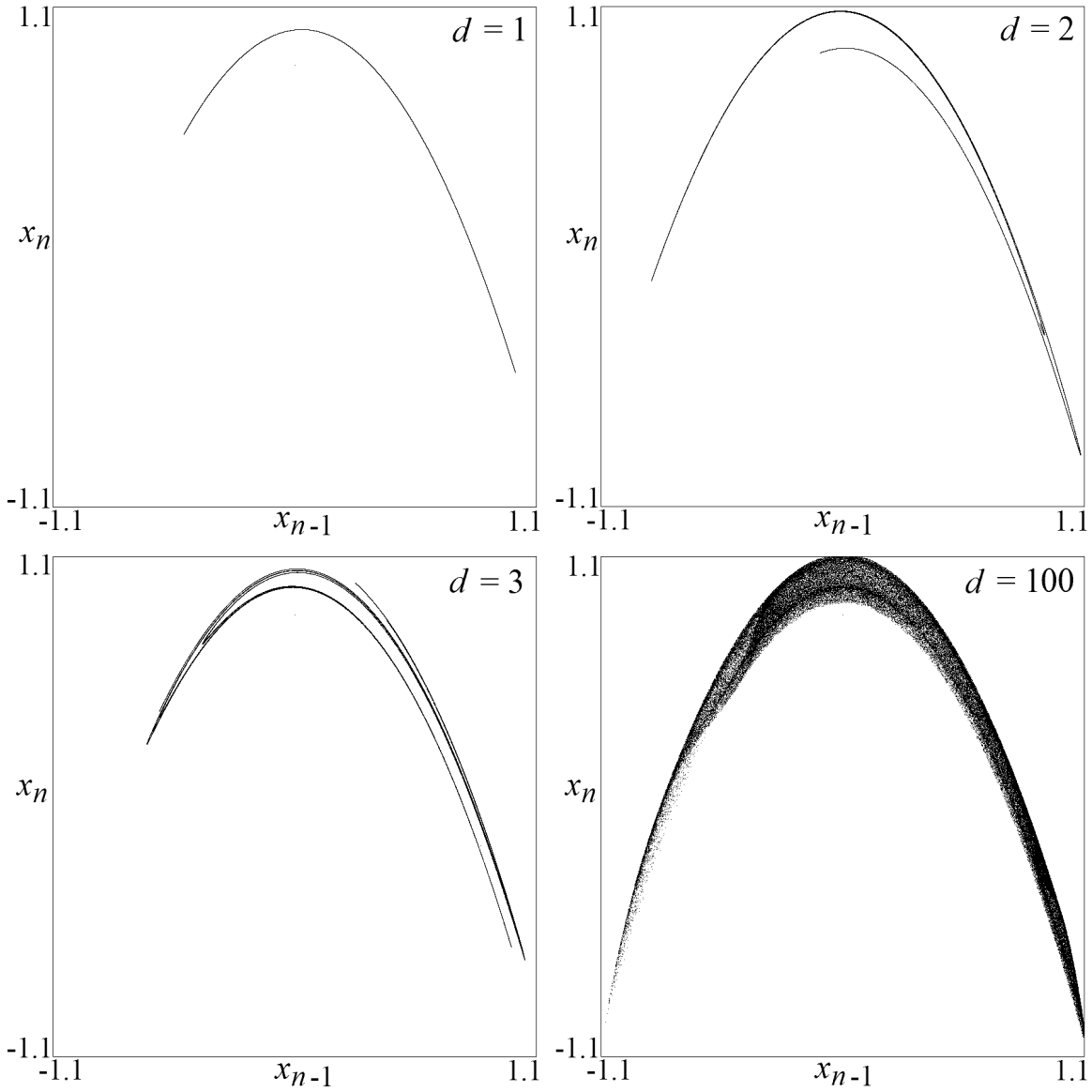

Fig. 2 Attractors for the system in Eq. (1) with $a = 1.6$ and $b = 0.1$ for various values of the time delay.

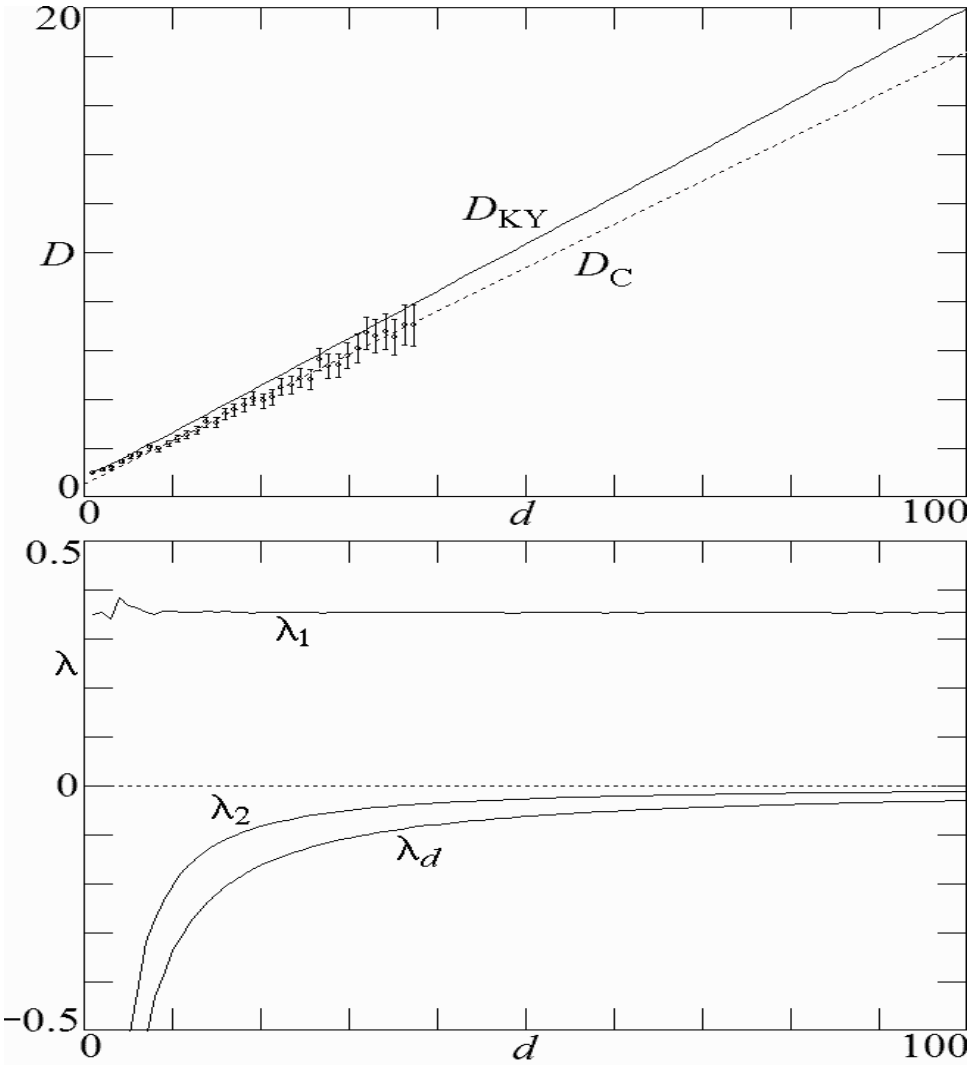

Fig. 3 Kaplan-Yorke dimension and Lyapunov exponents for the system in Eq. (1) with $a = 1.6$ and $b = 0.1$ versus time delay.

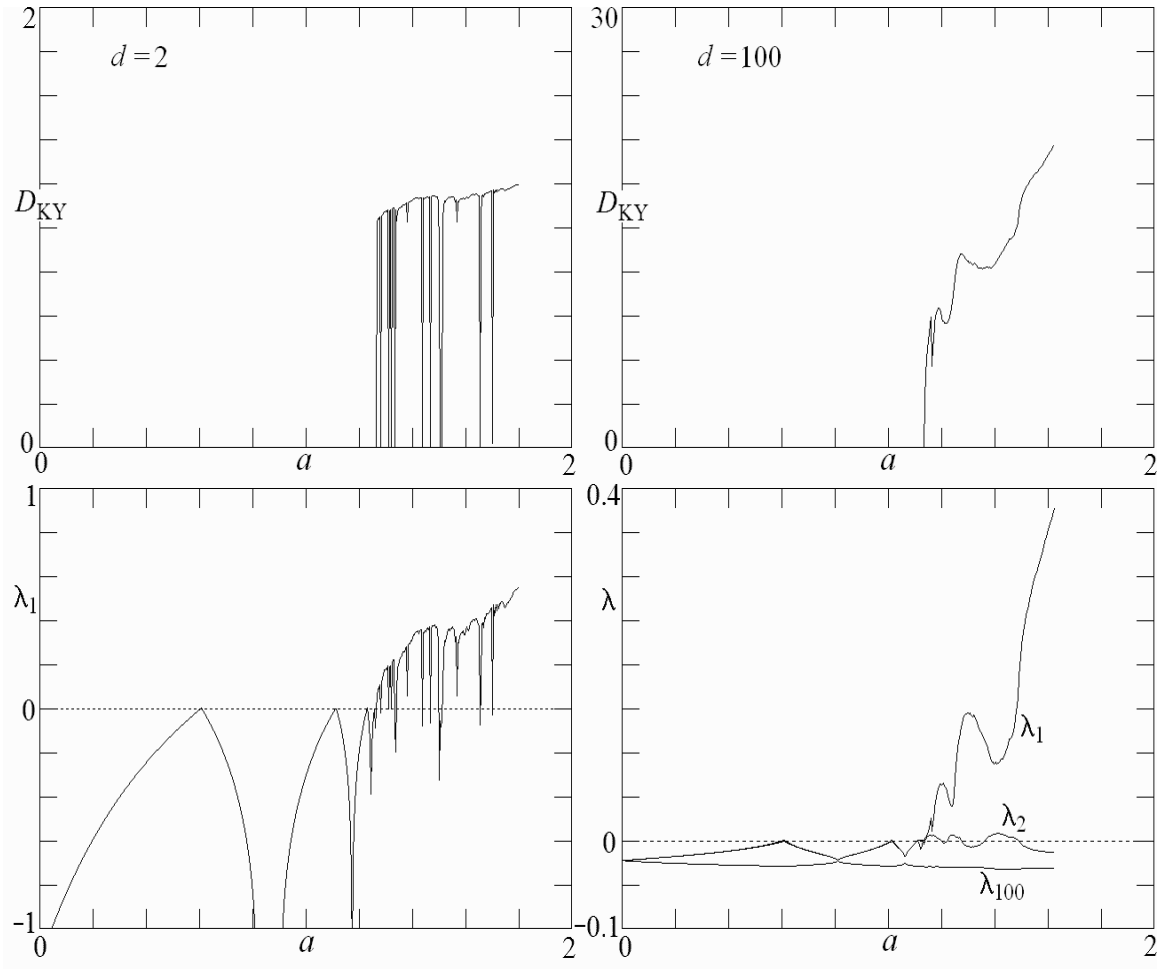

Fig. 4 Kaplan-Yorke dimension and Lyapunov exponents for the system in Eq. (1) with $b = 0.1$ showing the route to chaos at low dimension (d= 2) and high dimension (d = 100).

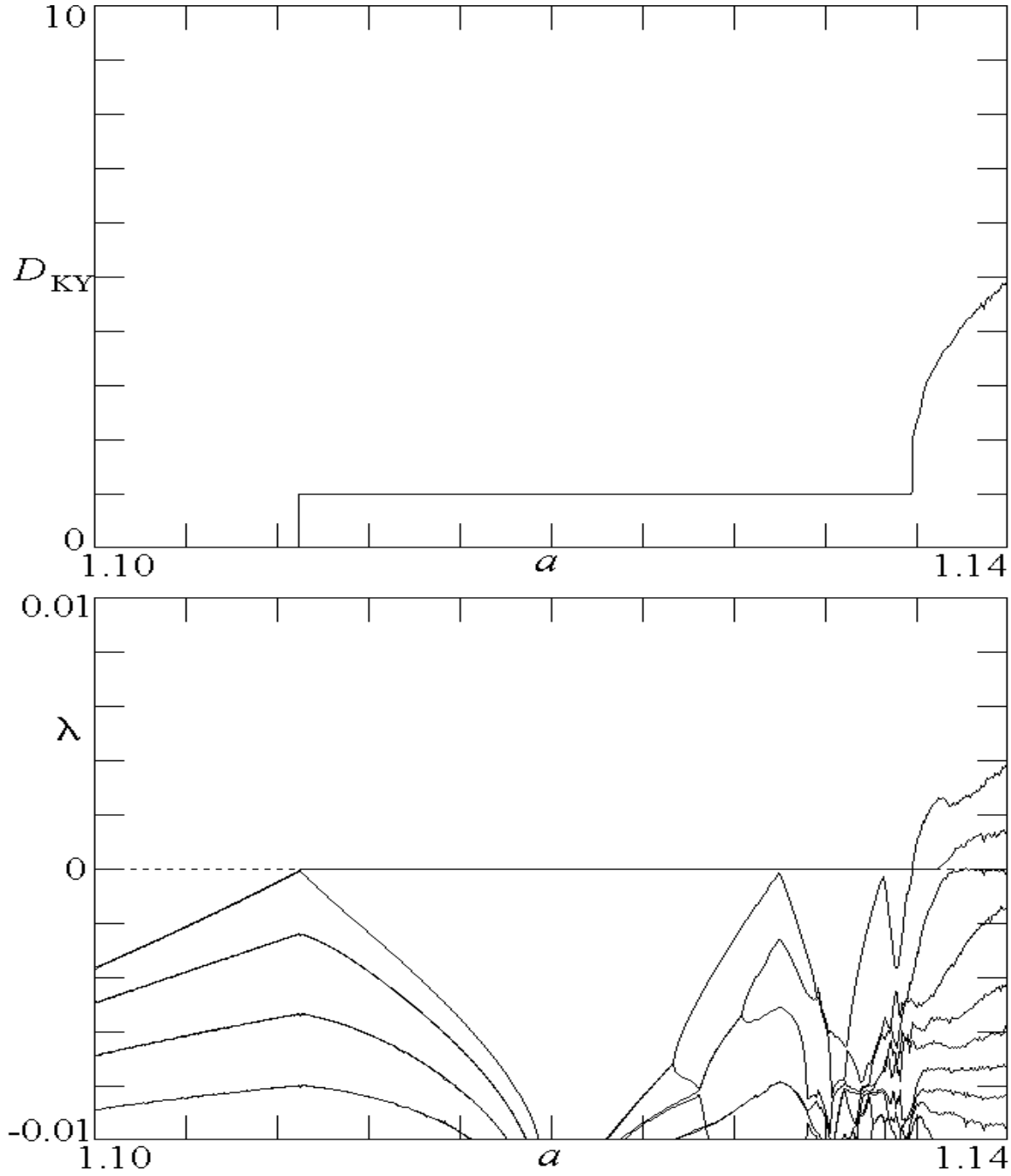

Fig. 5 Kaplan-Yorke dimension and a few of the largest Lyapunov exponents for the system in Eq. (1) with $b = 0.1$ and $d = 100$ showing in more detail the onset of chaos.

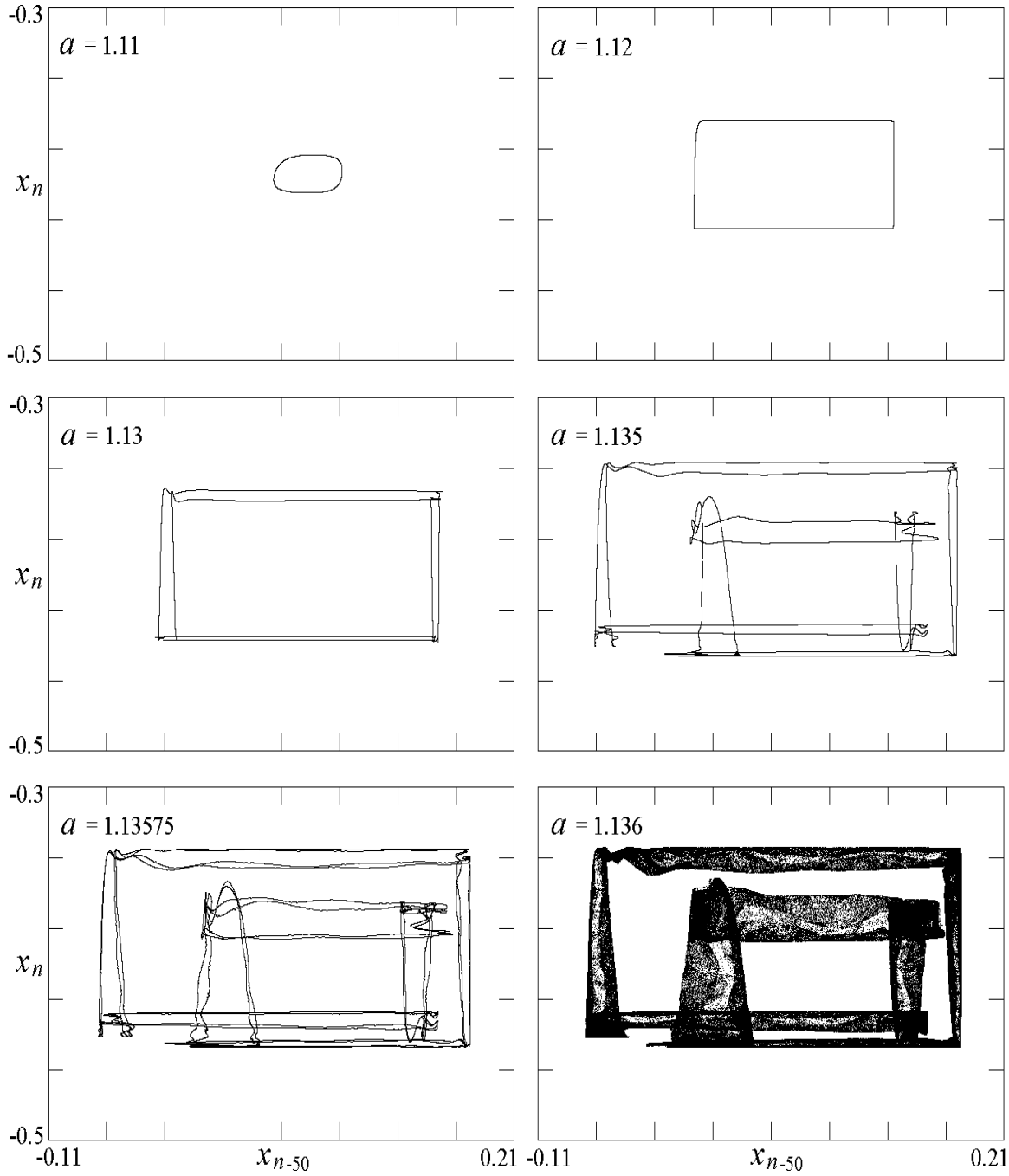

Fig. 6 Attractors for the system in Eq. (1) with $b = 0.1$ and $d = 100$ showing period doubling of a drift ring approaching the onset of chaos.

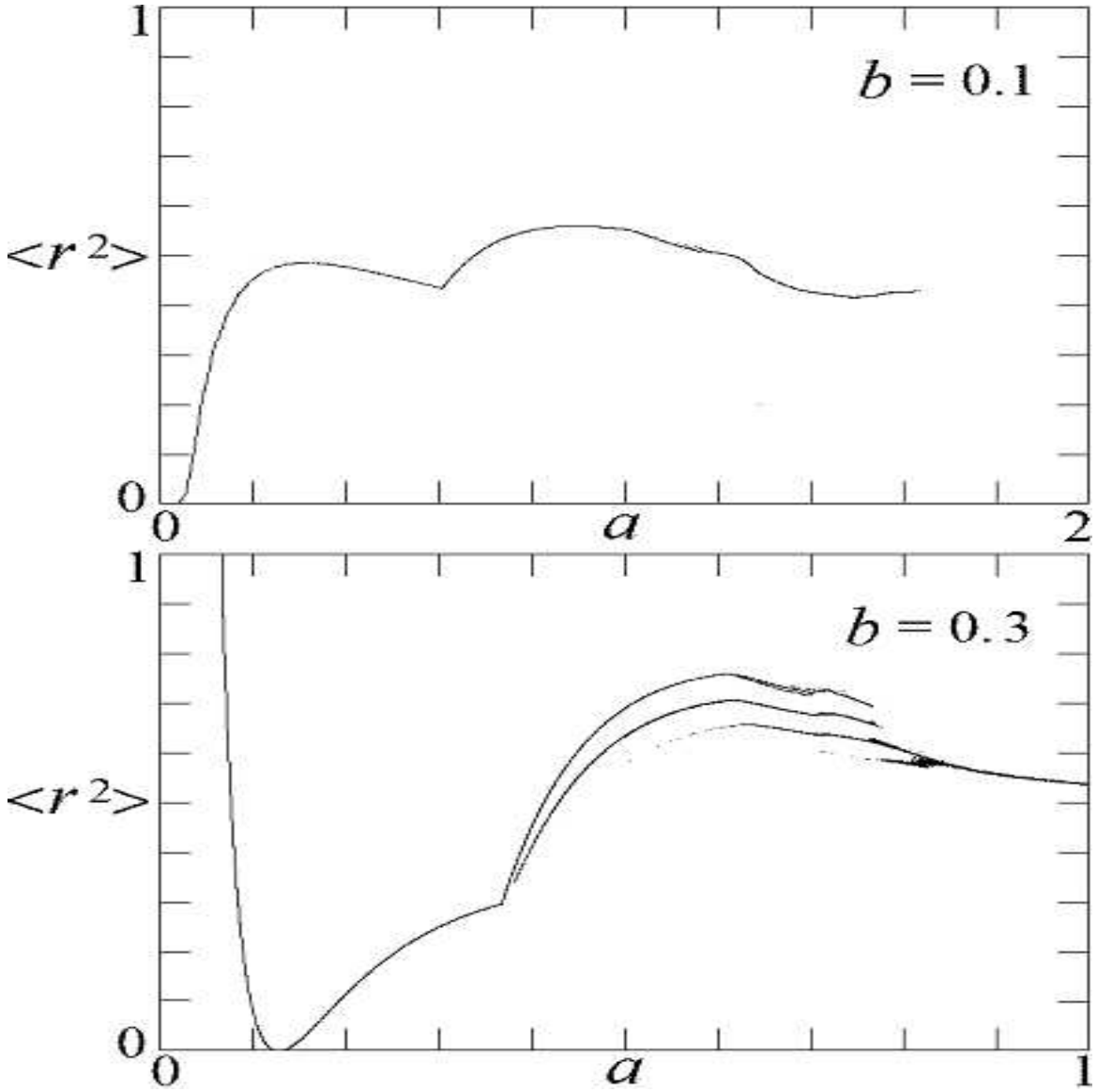

Fig. 7 Global bifurcations and multiple attractors for two values of b with $d = 100$.

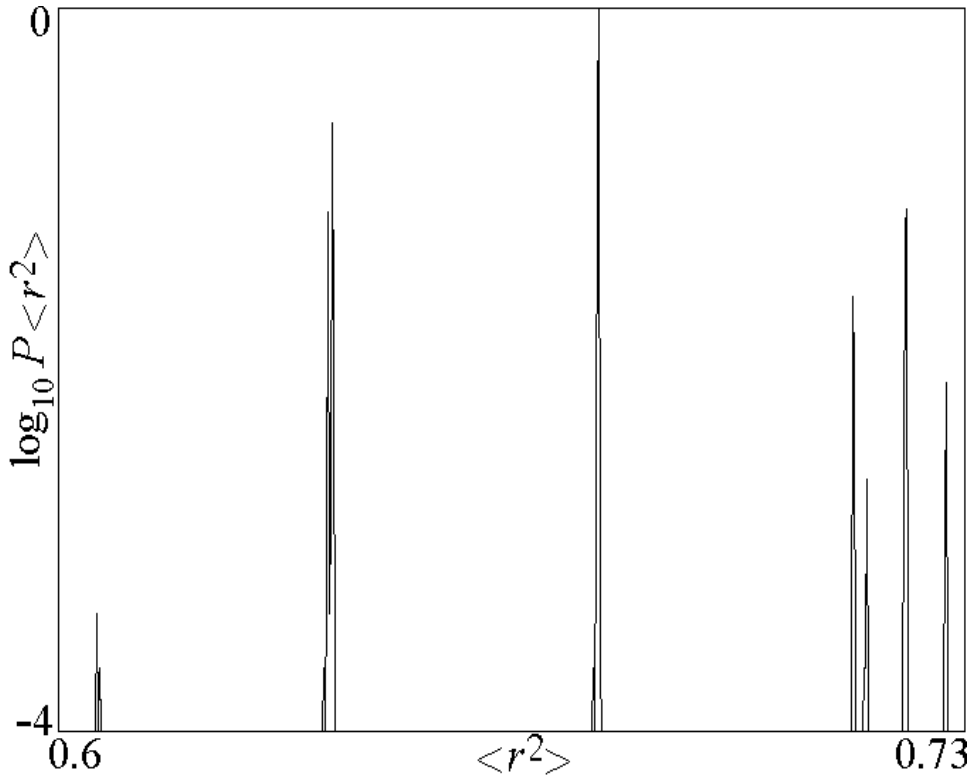

Fig. 8 Relative probability of different values of $\langle r^2 \rangle$ for $a = 0.7$, $b = 0.3$, and $d = 100$, indicating the existence of at least seven distinct attractors.

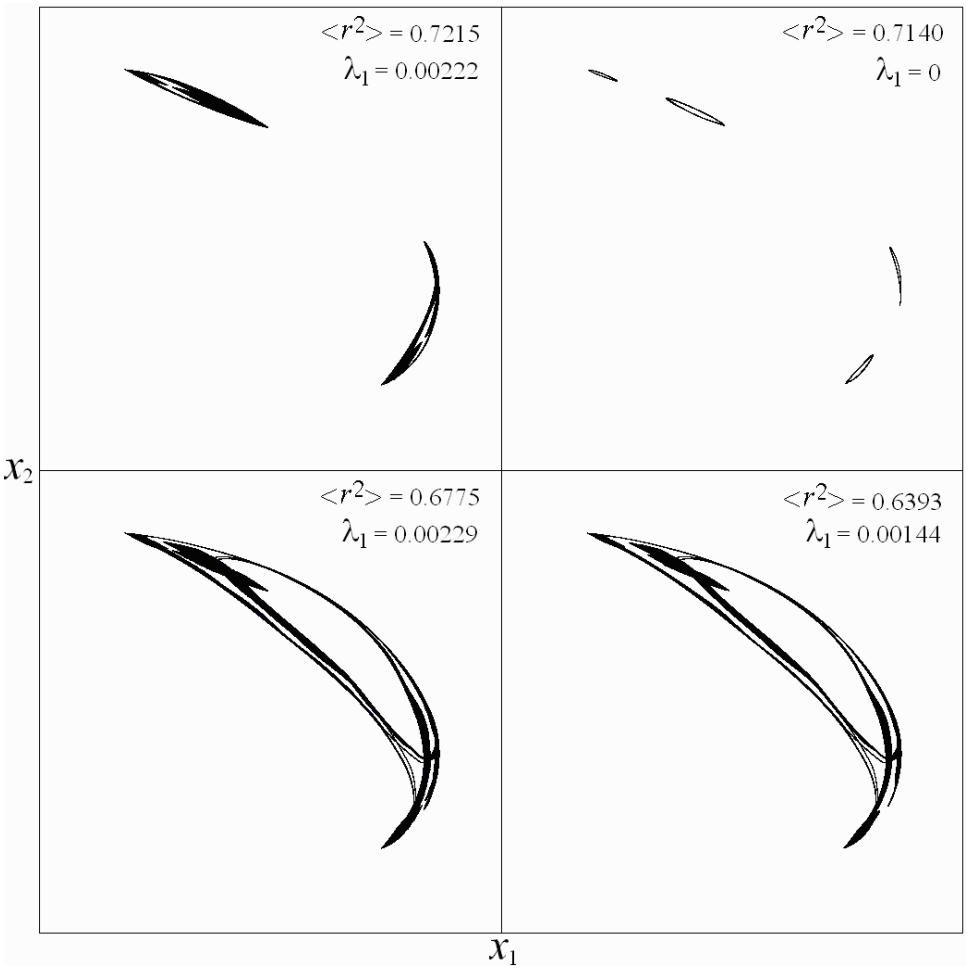

Fig. 9 Four coexisting attractors for $a = 0.7$, $b = 0.3$, and $d = 100$ near the onset of chaos.